



MAX-PLANCK-GESELLSCHAFT



Originally published as:

**“Photoelectron Spectroscopy of Polycrystalline Platinum Catalysts”**

Z. Paál, R. Schlögl and G. Ertl

J. CHEM. SOC. FARADAY TRANS., 1992, 88(8), 1179-1189

doi: 10.1039/FT9928801179

# Photoelectron Spectroscopy of Polycrystalline Platinum Catalysts

Zoltán Paál,\*† Robert Schlögl and Gerhard Ertl

Fritz-Haber-Institut der Max-Planck-Gesellschaft, Faradayweg 4-6, D-1000 Berlin 33, Germany

Pt black catalysts have been characterized by X-ray photoelectron spectroscopy (XPS) and ultraviolet photoelectron spectroscopy (UPS). The spectra measured after standard purification ( $O_2$  and  $H_2$  at 600 K) compared well with those of a purified reference Pt foil. All samples exhibited pronounced Fermi-edge intensities in UPS although only 60–70% Pt was detected on their surfaces by XPS, the remainder being C and O. Line analysis of the C 1s XPS region showed the presence of partly oxidized graphite and hydrocarbon polymer, likely in three-dimensional islands. OH/ $H_2O$  species attached to the metallic Pt sites were detected by UPS bands, in agreement with O 1s XPS line analysis. Similar spectral features are recorded at 600 K. Carbon could not be removed entirely by  $O_2$  up to 850 K; hydrogen did not remove surface oxygen even up to 750 K. UPS features of C on Pt used in hydrocarbon reactions were similar to those reported for amorphous hydrogenated carbon overlayers. Consequences of the present findings for the catalytic properties of Pt in *n*-hexane reactions and the quantification of  $H_2$ – $O_2$  titration are discussed briefly.

Surface spectroscopic methods for catalyst characterization<sup>1</sup> give information on the nature of the entire surface rather than on individual active sites. Well defined electronic states can be distinguished on homogeneous surfaces (*e.g.* single crystals and their adsorbed overlayers<sup>2</sup>). These systems are, as a rule, far from actual catalyst systems where one meets surfaces exposed to reactants at higher pressures and at elevated temperatures. The electron spectroscopic studies of real catalysts reported here represent another attempt to bridge the gap between surface science and catalysis.<sup>3</sup>

Platinum catalyses skeletal hydrocarbon reactions either in dispersed form<sup>4</sup> or as single crystals.<sup>5,6</sup> Unsupported platinum black exhibited catalytic selectivities analogous to single crystals under similar conditions.<sup>7</sup> This catalyst offers the possibility of obtaining related information on catalytic and surface properties.

The morphology and surface properties of Pt black have been studied by electron microscopy (EM),<sup>8,9</sup> XPS<sup>10</sup> and SIMS.<sup>11</sup> Carbon and oxygen impurities were detected by XPS together with Pt after lengthy storage of the catalyst in air.<sup>10</sup> The position of Pt 4f peaks did not indicate species other than Pt<sup>0</sup> although their asymmetry pointed to the presence of chemically bound moieties. Hydrogen treatment at room temperature removed some of these and reduced the surface Pt considerably.

The optimum procedure for combining surface chemical and catalytic investigations would be to use an *in situ* set-up to carry out catalytic reactions and previous/subsequent surface spectroscopy without exposure to the atmosphere.<sup>5,6</sup> The present study applies the 'next best' solution, *i.e.* the catalysts were introduced into the UHV system and thereafter they were treated in a preparation chamber without contact with air. The aim was: (1) to probe the possibilities of XPS and also UPS for the surface characterization of a polycrystalline, not sputter-cleaned metal powder in various states; (2) to simulate the purification ('regeneration') processes used in catalysis and thus characterize the state of the catalyst at its moment of contact with the reactant; (3) to compare the catalyst surfaces prior to and after chemical purification with that of a Pt foil purified mainly by chemical methods representing a chemically 'realistic' and practically useful reference state containing minor O and C impurities.

Most literature UPS data are related to adlayers formed at low exposures at clean surfaces. In such studies well defined patterns originating from molecular orbitals are obtained which can be rationalized by comparison with gas-phase UPS data. This approach is difficult in the present case since a variety of materials with different electrical conductivity creates a complex spectrum superimposed on a structured background of secondary electrons from the insulating parts of the surface. Besides the near-Fermi edge features characterizing the metallic part of the complex surface only rather general information about the adlayers are possible. They complement well, however, a line profile analysis carried out with selected C 1s and O 1s XPS signals. This method supplied valuable information on Pd black catalysts.<sup>12,13</sup>

## Experimental

### Sample Preparation and Pretreatment

Pt black catalysts were prepared by reduction of  $H_2PtCl_6$  in aqueous solution. One sample was reduced by HCHO in the presence of KOH<sup>9,10</sup> and pre-sintered in hydrogen at 473 and 633 K, respectively<sup>9</sup> (Pt-HCHO-473 and Pt-HCHO-633). Another Pt sample was reduced without the use of K, by boiling hydrazine (Pt-N). All samples were stored for several months in air; some were used as catalysts in hydrocarbon reactions. A Pt foil of nominal purity 99.99% was used as a reference. This was cleaned *in situ* by repeated  $Ar^+$  ion bombardment and oxidation at 720 K. In the final purification stages, oxidation was followed also by hydrogen treatment. After repeating the cycle several times, segregation of impurities (mainly C) from the bulk completely ceased. The fine grain structure with its boundary impurities was the final limiting factor, prohibiting perfect cleaning.

The standard purification of Pt blacks consisted of contact with 26 mbar  $O_2$  for 3 min followed by a 5 min evacuation and 263 mbar  $H_2$  for 10 min at 603 K in the preparation chamber. This procedure was analogous to that used between runs of hydrocarbon reactions.<sup>7,9</sup>

### Apparatus

The UHV system consisted of two consecutive preparation chambers with an individual pumping system allowing transfer of samples rapidly into UHV without contamination after gas treatments at pressures up to 1 bar. Powder samples of

† Present address: Institute of Isotopes of the Hungarian Academy of Sciences Budapest, P.O.B. 77, H-1525 Hungary.

ca. 10 mg were placed into the cavity of a pre-cleaned boat of stainless steel. This was fixed to a manipulator rod SRT-11 which permitted one-dimensional motion from atmosphere through two antechambers to the UHV vessel. The sample section of this rod could be temperature controlled from 75 to 1000 K. The temperature was measured within the rod, ca. 3 mm below the centre of the sample by a thermocouple.<sup>14</sup> A mass spectrometer allowed monitoring of the purity of the gases used (nominal purity, 99.9996%).

The analysis chamber was equipped with a Leybold EA-12 analyser and sources for XPS, UPS, AES and ISS. The angle of incidence was 30°, the entrance slit of the analyser was parallel to the sample surface. The base pressure was  $8 \times 10^{-11}$  mbar. With a sample under analysis, the pressure was ca.  $10^{-9}$  mbar with a large fraction of the residual gas being H<sub>2</sub>.

### Procedure

XPS measurements were carried out using Mg-K $\alpha$  excitation (1253.6 eV) with the analyser in the pass energy mode (PE = 50 eV). The retard ratio mode (RR = 4) was used for survey spectra. The energy scale was calibrated to Au 4f<sub>7/2</sub> = 84.0 eV. A Leybold DS-100 software system was used for spectrum processing (smoothing, background subtraction and integration as well as for curve fitting).<sup>13,15</sup> A Shirley-type background was assumed except for minor components (K < 1%) where a linear background seemed more adequate. UP spectra were taken with He I (21.2 eV) and He II (40.8 eV) excitation with pass energies of 4 eV and 20 eV, respectively. The DS-100 software allows calculation of difference spectra without or with intensity normalization.

### Processing and Assignment of XP Spectra

Individual components were fitted to the smoothed O 1s and C 1s lines. A mixture of Lorentzian and Gaussian curves<sup>14</sup> (1 : 5) was used, with fixed FWHM values and a predetermined number of peaks. Peak positions and intensities remained variable parameters to be found by the program itself. Such a fitting process has always some arbitrary character, since a solution with physico-chemical meaning is expected as a result of a pure mathematical procedure which may result from more than one best fit within the acceptable limit of error. Several dozen samples were fitted with various initial parameters and the 'self-consistency approach' was used to find most likely and also chemically meaningful peak assignments. The binding energy ( $E_b$ ) values of the resulting peak positions are satisfactorily reproducible for different samples. It is sometimes difficult to find small peaks in the direct vicinity of large contributions.<sup>16</sup> Therefore, peak  $E_b$  positions were also fixed for small PtO and PtC peaks. The computer program indicated 'no physical reality', for those peaks when they were really absent.

Selected literature  $E_b$  values for oxygenates, sorbed species<sup>16-22</sup> or polymer films,<sup>23,24</sup> are shown in Table 1. For C 1s, results obtained on graphite samples,<sup>15,25,26</sup> hydrocarbons sorbed on metals,<sup>27</sup> amorphous hydrogenated carbon overlayers (a-C : H)<sup>16,28,29</sup> and polymer films [polyimides, poly(vinyl alcohol)]<sup>23,24,30</sup> as well as coke on a Zr phosphate catalyst<sup>31</sup> can be used as reference (Table 2). Single-bonded oxygen atoms (like C—O—H, C—O—C) cause a chemical shift relative to graphite of ca. 1.5 eV while bands arising from double bonds (like C=O) are shifted 3–3.5 eV towards higher  $E_b$  values.<sup>25,26</sup> The C 1s peak of oxidized carbon samples, showed also a characteristic increase in FWHM values.<sup>26</sup>

**Table 1**  $E_b$  values of O 1s peak of surface oxygen in various chemical states

| species                              | $E_b$ /eV                   | ref.   |
|--------------------------------------|-----------------------------|--------|
| subsurface O/Pt                      | 530                         | 17     |
| PtO                                  | 530.2                       | 19     |
| O on K-doped Pt                      | 530.9                       | 20     |
| PtOH                                 | 531.5 $\pm$ 0.5             | 19     |
| O atoms on Pt (or SiO <sub>2</sub> ) | 531.6                       | 17     |
| CO/Pt(111) + K                       | 531.3                       | 21     |
| CO/Pt(111)                           | 531.0 (bridged)             | 21     |
|                                      | 532.7 (on-top)              | 21, 22 |
| H <sub>2</sub> O/Pt                  | 532.2 to 532.9 <sup>a</sup> | 20     |
| H <sub>2</sub> O/O(ads)/Pt(111)      | 532.3                       | 18     |
| carbonyl CO                          | 532.0                       | 23     |
| adsorbed O on Pt                     | 533                         | 22, 34 |
| SiO <sub>2</sub> islands on Pt foil  | 533.1                       | 17     |
| C—O—H                                | 533.4                       | 24     |
| C—O—C                                | 533.6                       | 23     |

<sup>a</sup> Shifting to higher  $E_b$  values with increasing water coverages.

We used an FWHM of 1.8 (or, for PtO, 1.7) eV<sup>24</sup> for fitting individual components to the O 1s and an FWHM of 1.3 eV for C 1s curve fitting, both following thin polymer film data.<sup>24</sup>

The Pt 4f line is a doublet with an inherent, pronounced asymmetry towards the higher  $E_b$  side arising from final-state effects.<sup>32</sup> Pt oxides have higher  $E_b$  values than the pure metal (with counter claims as far as their nature and exact  $E_b$  values are concerned<sup>19,33,34</sup>). Onsetting oxidation appears first as an increased asymmetry towards higher  $E_b$ .<sup>19,33,34</sup> This asymmetric tail has been even entirely attributed to Pt interacting with adsorbed O.<sup>33</sup> Another approach<sup>34</sup> resolved the asymmetric peak of metallic Pt into a main and satellite component. Upon electrochemical oxidation, other tail peaks appeared, due to Pt<sup>2+</sup> and Pt<sup>4+</sup>. The area of the main peak relative to the sum of these 'tail' lines was found to be rather sensitive to the degree of Pt oxidation. We fitted components to the Pt 4f region so as to achieve a good fit to the measured spectrum (low residual chi values). The FWHM values and the 7/2 to 5/2 ratio for the Pt metal component have been taken from the literature.<sup>33</sup> No physical meaning was attrib-

**Table 2**  $E_b$  values of various C 1s contributions belonging to carbon in various chemical states

| species  | $E_b$ /eV   | ref.   |
|--|-------------|--------|
| carbide C:   |             |        |
| a-C : H overlayer                                      | 283.0       | 28     |
| ethynylidyne ('Pt <sub>3</sub> C')                     | 283.4       | 27     |
| C atoms on Pt  | 283.9       | 16     |
| SiC  | 283.4       | 29     |
| graphitic C  |             |        |
| various graphite samples                               | 284.1–284.5 | 15     |
| Pt/C <sub>2</sub> H <sub>4</sub> , ads annealed 1130 K | 284.3       | 27     |
| graphite on Pt   | 284.7       | 16     |
| coke on Zr phosphate catalyst                          | 285.2       | 31     |
| C <sub>x</sub> H <sub>y</sub> polymer in a-C : H       | 285.3       | 16     |
| CH <sub>2</sub> groups in poly(vinyl alcohol)          | 285.0       | 24, 30 |
| 'unidentified polymer' on Pt                           | 285.9       | 29     |
| adsorbed CO  |             |        |
| on Pt  | 285.9       | 16     |
|  | 286.9       | 21     |
| on K doped Pt  | 285.8       | 21     |
| C—O—C groups in polymer films                          | 285.6–285.8 | 30     |
| oxidized a-C : H                                       | 286.5       | 28     |
| C—OH groups in poly(vinyl alcohol)                     | 286.5       | 24, 30 |
| C=O groups in poly(vinyl alcohol)                      | 287.8       | 24, 30 |
| in oxidized coke                                       | 287.9       | 31     |
| CO <sub>2</sub> H groups in poly(vinyl alcohol)        | 289.2       | 24, 30 |

**Table 3**  $E_b$  values for UP spectra of oxygenates on Pt surfaces

| species                    | T/K     | excitation source | $E_b$ /eV            | O 1s $E_b$ /eV | ref. |
|----------------------------|---------|-------------------|----------------------|----------------|------|
| O/Pt(100)                  | 300     | He I              | 3–4; broad 6–8       | —              | 35   |
| O/Pt foil                  | 273     | He II             | broad 6.1            | 533            | 22   |
| ox. Pt foil                | 273     | He I              | 5.5; 7.7; 9.2        | —              | 36   |
| O <sub>2</sub> /Pt(111)    | 100     | He II             | broad at ca. 8       | —              | 37   |
| O/Pt(111)                  | 300     | He I; He II       | ca. 5                | —              | 37   |
| O/Pt(111)                  | 100–300 | He II             | broad 5–7            | —              | 38   |
| OH/Pt(111)                 | 300     | He II             | 7.8; 11.1            | —              | 38   |
| OH/Pt(111) + K             | 326     | He I              | 4.7; 8.7             | 530.9          | 20   |
| H <sub>2</sub> O/Pt(111)   | 100     | He I              | 6; 8.1; 12           | 532.2–532.9    | 20   |
| H <sub>2</sub> O/K/Pt film | 135     | He II             | 7.3; 8.7; 11.3; 14.6 | 535.4          | 39   |
| OH on H <sub>2</sub> O     | 250–400 | He II             | 6.6; 10.3            | —              | 39   |
| CO/Pt(111)                 | 160     | He II             | 9.2; 11.7            | —              | 21   |
| CO/Pt(111) + K             | 160     | He II             | 8.9; 11.7            | —              | 21   |

**Table 4** UPS features of carbon-containing species

| species                                     | T/K | excitation source | $E_b$ /eV             | ref. |
|---|-----|-------------------|-----------------------|------|
| C <sub>2</sub> H <sub>4</sub> /Pt(111)      | 300 | He I              | 7.6; 8.2; 12.0        | 41   |
|   | 500 |                   | none                  |      |
| C <sub>2</sub> H <sub>4</sub> /Pt(111) + Cs | 200 | He I              | 7.3; 8.7              | 41   |
|   | 300 |                   | broad 7–8             |      |
| C <sub>6</sub> H <sub>5</sub> OH/Pd(110)    | 80  | He I              | 3.5–5; 6.5; 8.5; 12.5 | 42   |
|   | 300 |                   | 4.5; 6.5; 7.5; 11     |      |
|   | 500 |                   | broad, weak 5–11      |      |
| graphite                                    | 300 | He I              | weak 5; 9             | 15   |
|   |     | He II             | (3); 8                |      |

uted to the fitted tail components. Since onset of oxidation appears as shoulders in the tail region, the 'main-to-tail' ratio was used as a semiquantitative parameter to characterize the surface state of Pt.

### Characteristics of UP Spectra

Difference spectra are useful to extract peaks of molecular adsorbates. He I intensities were normalized to the conduction band maximum of Pt at 2.45 eV. The quality of the He II data was less adequate for difference spectra owing to the poor photoemitting properties of a loose powder sample. He I data are intense but are severely affected by secondary electron effects. He II data are weaker but are much less affected by secondary electrons. They allow probing of deep lying valence orbitals with reasonable emission intensities.

Reference spectral features of oxygenates adsorbed on Pt<sup>20–22,35–39</sup> are listed in Table 3. A peak at  $E_b = 5.5$  eV was attributed to dissolved O in Pd black;<sup>12</sup> upon hydrogen treatment, this segregates to the surface with  $E_b$  shifted to 5.8 eV. Intense hydrogenation resulted in OH signals at ca. 6.5 eV. The oxygen–hydrogen reaction on metal surfaces was shown, indeed, to be a slow process.<sup>40</sup>

UPS bands<sup>14,41,42</sup> of carbon-containing adspecies exhibit sharp and well defined bands at low temperatures only (Table 4); all of them tend to disappear upon even moderate heating.<sup>42</sup> UP spectra of a-C:H overlayers contain a broad band between 4 and 12 eV;<sup>43</sup> those reported for polyimide monolayers<sup>44,45</sup> exhibit, in addition, a smaller maximum at ca. 6 eV, together with a broad band between 8 and 12 eV.

Adsorption of hydrogen at 80 K on Pt(111) decreased the intensity near the Fermi edge and increased slightly the intensity at ca. 4 eV. It gave rise to new features at 6.4 and 7.3 eV as detected by both He I and He II excitation.<sup>46</sup>

Of the possible impurities, as a rule, oxygen-containing species are expected to produce intense UPS signals rather than carbonaceous ones. Exact positions were reported to depend on the presence of surface impurities (*e.g.* K<sup>+</sup>, SiO<sub>2</sub>

*etc.*)<sup>20,36</sup> and heating can also cause  $E_b$  shifts up to 1–1.5 eV (Tables 3 and 4).

## Results and Discussion

### Reference Experiments

Literature recommends purification of Pt foil by heating to 1000 K or above.<sup>47</sup> Such treatment is inappropriate for powdered catalyst samples and thus all heating was limited to ca. 750 K. In this way not all impurities were removed from the foil which will be referred to as 'purified'. The first sputtering removed silica impurities. Four final stages of purification will be presented for Pt foil. Case 1 involved a treatment with two 5 min O<sub>2</sub> (14 mbar) at 483 K followed by 2.5 h of Ar<sup>+</sup> sputtering (1 kV,  $1 \times 10^{-5}$  mbar Ar). This surface was subsequently hydrogen treated (67 mbar) at 603 K for 5 min (case 2). Case 3 was obtained after a 'standard regeneration' (see Experimental). A final H<sub>2</sub> treatment (67 mbar at 483 K) followed by sputtering for 70 min at 300 K led to the state of case 4. The atomic compositions are summarized in Table 5. The work function values were obtained from the low-energy cut-off of the UP spectra.<sup>22</sup>

The Pt 4f line proved to be insensitive in position and shape to any of these treatments and indicates only metallic

**Table 5** Composition of Pt foil after various treatments measured by XPS

| sample no.               | composition (atom%) <sup>a</sup> |    |    | $\Phi$ /eV |
|--------------------------|----------------------------------|----|----|------------|
|                          | O                                | C  | Pt |            |
| as received <sup>b</sup> | 12                               | 52 | 13 | 4.8        |
| case 1                   | 3                                | 10 | 87 | 5.0        |
| case 2                   | 2                                | 13 | 85 | 5.1        |
| case 3                   | 9                                | 9  | 82 | 5.0        |
| case 4                   | 4                                | 8  | 88 | 5.1        |

<sup>a</sup> Calculated from the peak areas of O 1s, C 1s and the Pt 4f doublet using the atomic sensitivity factors stored in the memory of the DS-100 software (O: 0.61; C: 0.20; Pt: 3.1). <sup>b</sup> Plus 23% Si.

Pt with Pt 4f<sub>7/2</sub>  $E_b$  of 71.1 eV, being in fair agreement with literature values.<sup>10</sup> The main-to-tail peak ratio was 69 : 31 in good agreement with the ratios of (68–70) : (32–30) reported for electrochemically purified Pt.<sup>34</sup> Neither this nor the peak shape showed any sign of surface oxidation.<sup>19</sup>

It is illustrated in ref. 14, how the O 1s and C 1s bands are decomposed into individual components. No PtO ( $E_b \approx 530.2$  eV) was detected in the O 1s spectra of the reference Pt foil. The peak at ca. 531.5 eV was assigned to OH groups<sup>14,20</sup> while that at ca. 532.5 eV indicates the presence of water.<sup>20</sup> A peak at ca. 536 eV may correspond to the oxygen content of oxidized surface carbon.<sup>23,24</sup> Minor peak(s) at still higher  $E_b$  may correspond to higher oxidation states of the three-dimensional (3D) carbon or to charged species, e.g. water adsorbed on those insulating patches.<sup>16</sup>

The C 1s band contains two large contributions, one at 284.3–284.6 eV and another above 285 eV. We attribute the former to 'graphite', the latter to a hydrocarbon polymer. Most of the carbon overlayer may be present at grain boundaries. Scanning photoemission microscopy<sup>48</sup> also demonstrated differences between the oxygen adsorption ability of different crystal faces in one single polished plane. The inhomogeneities observed along grain boundaries may be due to the enrichment of carbon at those sites.

One must not regard these carbonaceous species as well defined chemical entities. Instead, a stack of carbonaceous material has to be assumed, containing aromatic rings (sp<sup>2</sup> C atoms) denoted graphite as well as aliphatic chains (sp<sup>3</sup> C atoms) representing the 'C<sub>x</sub>H<sub>y</sub>' species. Both of them can contain oxygen atoms in a single or double chemical bond (peaks at around 286 and above 287 eV). Quinone structures were reported to be present in a coke overlayer of a styrene dehydrogenation oxide catalyst.<sup>31</sup> Decomposition of the resulting spectrum into individual lines supplies semi-quantitative information on those moieties rather than a possibility of their separation to well defined adspecies.

One has to bear those in mind when the amounts of the individual O 1s and C 1s contributions in cases 1–4 are compared (Fig. 1). The main body of oxygen (45–60%) is present as water together with some OH groups. The relative abundance of the oxidized carbon is low; its amount estimated from the corresponding O and C signals is in fair agreement. Oxygen and hydrogen treatment at elevated temperatures ('catalyst regeneration', cases 3 and 4) removes first C–O components of the C 1s peak; at the same time, the relative amount of both OH groups and H<sub>2</sub>O increase. Regeneration by O<sub>2</sub> and H<sub>2</sub> in case 3 gave rise to carbon oxidation to C=O groups; these are removed in case 4.

UP spectra indicate a cleaner surface than one should conclude from XPS. The spectrum after treatment 2 (Fig. 2) is closest to that reported for pure Pt.<sup>46</sup> The difference spectrum (case 1) – (case 2) indicates the presence of small amounts of CO in case 1 arising as contamination during lengthy sputtering. The difference spectrum (case 3) – (case 2) exhibits two rather flat bands which indicate the presence of OH and water after contact with H<sub>2</sub> and O<sub>2</sub>.<sup>20,38</sup> The presence of CO decreases the height of the Fermi edge as opposed to OH/H<sub>2</sub>O (at least in their form stable at 326 K). Assignment of the band at  $E_b$  6 eV to atomic oxygen<sup>16,37</sup> is not likely since this would involve an intensity loss in the Pt conduction band. The UPS signals are in agreement with XPS results showing enhanced bands at 531.5 (OH) and at 532.5 eV (H<sub>2</sub>O) for case 3. CO overlapping with other C 1s components cannot be identified in XPS. The work function values are close to that reported for clean Pt<sup>22</sup> ( $5.3 \pm 0.15$  eV).

The shape of the He I spectrum of purified Pt (Fig. 2) closely resembles that reported after hydrogen adsorption at

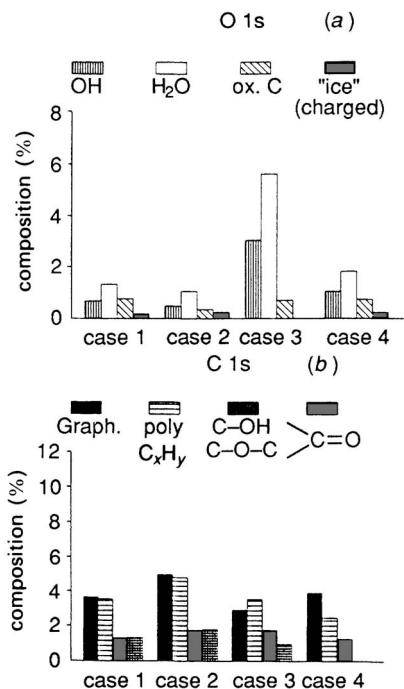


Fig. 1 Bar graphs of individual O 1s and C 1s contributions measured for Pt foil in cases 1 to 4 (Table 5), expressed as percentages of the total surface composition (O 1s + C 1s + Pt 4f = 100%)

low temperature.<sup>46</sup> The highest Fermi-edge intensity (cleanest metallic state) is obtained where the amount of oxygen is minimum rather than where the amount of exposed Pt is maximum (Table 5). This state was achieved after the first contact of Pt foil with hydrogen, underlining the importance of hydrogen in surface purification. Carbon exists mostly as a carbonaceous 3D overlayer and does not seem to interact electronically with the Pt surface (except for CO).

The He II spectra are close to literature data.<sup>49–51</sup> The presence of CO in case 1 is confirmed. The sharp band between  $E_b$  0 and 5.5 eV in the He II spectrum obtained with single crystals<sup>50,51</sup> arising from surface states cannot be expected to be reproduced here.

The information provided by XPS and UPS is basically complementary. It is remarkable that a polycrystalline Pt sample could be purified to a very large extent at moderate

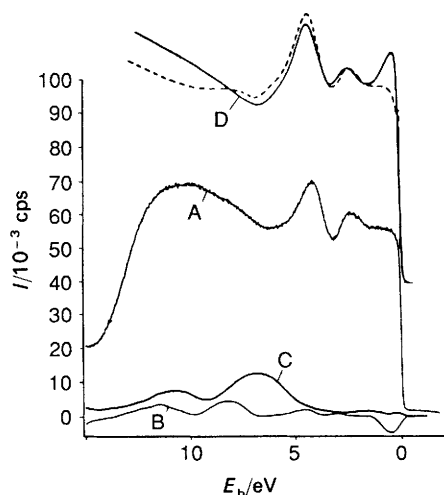


Fig. 2 A, UP He I spectrum for the reference Pt foil (case 2); B, difference spectrum case 1 – case 2; C, difference spectrum case 3 – case 2; D, curves reported<sup>46</sup> for Pt(111) (full line) and Pt(111) plus sorbed hydrogen (dashed line)

temperatures, mainly by a chemical treatment that is similar to regenerative catalyst cleaning.

### Photoelectron Spectroscopy of Purified Pt Black Samples

Pt black samples (Pt-N, Pt-HCHO-473 and Pt-HCHO-633) will be compared in their clean state, *i.e.* after standard regeneration as described in the Experimental section. This procedure was applied in case 3 for the Pt foil (Fig. 1). Note that several sputtering steps preceded this treatment in the reference case and the sample purity was, hence, higher. Attempts to sputter-clean the Pt black samples, however, were detrimental to the surface composition.

The O 1s, C 1s and Pt 4f lines in XPS show essentially similar features as in the case of Pt foil. In addition, up to 2% K is also present in the samples reduced by KOH-HCHO, as identified by XPS lines similar to those reported for Pt with K<sup>20</sup> and KOH<sup>52</sup> added. Pt-N contains only traces of K. Potassium can stabilize the adsorbed O and OH species<sup>20</sup> and shift the position of the adsorbed CO peak in UPS;<sup>21</sup> this will be borne in mind when discussing XP and UP spectra.

Compositions as calculated from XPS [Table 6(a)] show that Pt-N is the cleanest of all samples. As for the work function, oxygen adsorption increases,<sup>22</sup> hydrocarbon adsorption decreases<sup>53</sup> its value. The measured value is, therefore, a consequence of these effects.

The main-to-tail ratios of the Pt 4f contributions are close to the values observed with the reference foil and indicate clean metal as the predominant species.

A small peak corresponding to PtO appears in the O 1s band in each case (Fig. 3). *Ca.* 6% PtO (related to the total surface) in Pt-N causes a just detectable shift in the main-to-tail ratio of the Pt 4f region [Table 6(a)] while no such effect is seen with *ca.* 3.5% PtO over the two Pt-HCHO samples. Hence the detection of PtO seems to be less sensitive in the Pt 4f region where small Pt oxide peaks are suppressed by the intensive tail component of the Pt<sup>0</sup> line. The amounts of oxidized C and the charged species are higher with the two Pt-HCHO samples (particularly after sintering at 633 K) than with Pt-N. No signal attributable to subsurface oxygen atoms (529.5 eV) is observed, hence their amount is not significant, unlike palladium black.<sup>12,13</sup>

Small amounts of Pt-C are seen in two cases on the C 1s spectra. The main body of carbon consists of graphite and hydrocarbon polymer, the latter being present in higher amounts. The relative amount of oxidized carbon is higher

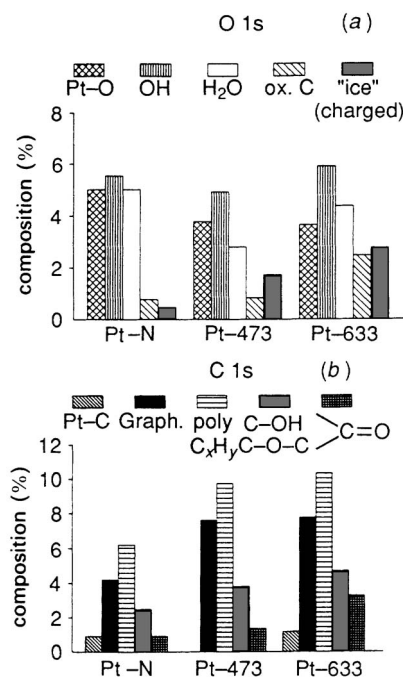


Fig. 3 Bar graphs of individual O 1s and C 1s contributions measured for Pt-N and two Pt-HCHO samples, expressed as percentages of the total surface composition (O 1s + C 1s + Pt 4f = 100%)

on the blacks than on the foil (as seen also in the O 1s region) and is almost independent of the previous exposure of the Pt to hydrocarbon reactants. Regeneration seems to reduce initial differences. A small contribution due, likely, to carbon-yllic C=O groups ( $E_b \approx 287.5$  eV) also appears.

He I UP spectra are shown in Fig. 4. The difference spectra (reference Pt minus Pt black) show more pronounced metallic valence states ( $E_b$  0–5 eV) in the Pt foil since the emission is obviously more intense from a compact sample than from a loose powder. Nevertheless, the resemblance of the Pt black spectra to that of a spectrum reported for a clean Pt foil<sup>54</sup> is obvious.

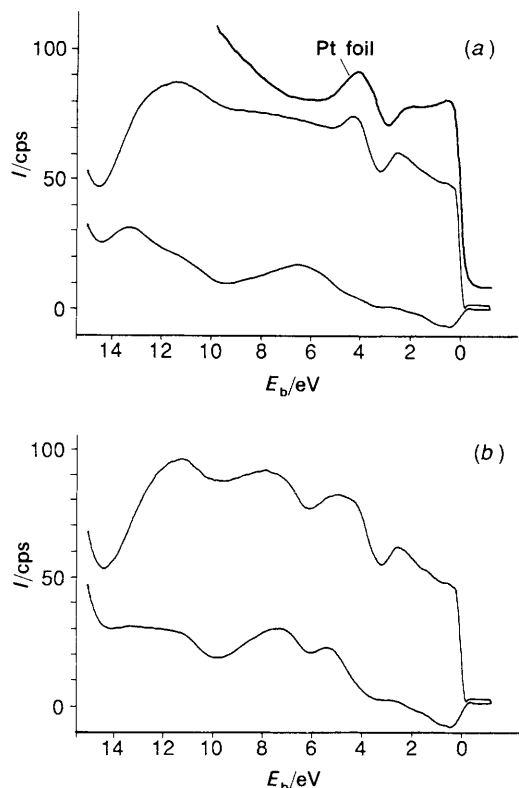
The difference spectrum between the reference Pt foil and Pt-N shows a rather featureless broad band between 4 and 10 eV. This must contain the contributions of several oxygenated species. The broad band at *ca.* 13 eV is due to water. All

Table 6 Composition of Pt black samples after various treatments<sup>a</sup>

| sample   | composition (atom%) |   |    |    | $\Phi$ /eV | Pt 4f area in |      |
|--|---------------------|---|----|----|------------|---------------|------|
|  | O                   | K | C  | Pt |            | main          | tail |
| peak (%)   |                     |   |    |    |            |               |      |
| <i>(a)</i> clean catalysts                                     |                     |   |    |    |            |               |      |
| 1 Pt-N <sup>b</sup>  | 17                  | — | 15 | 68 | 5.1        | 67            | 33   |
| 2 Pt-HCHO-473 <sup>c</sup>                                     | 14                  | 2 | 22 | 62 | 4.4        | 68            | 32   |
| 3 Pt-HCHO-633 <sup>c</sup>                                     | 18                  | 2 | 29 | 51 | 4.4        | 68            | 32   |
| <i>(b)</i> as received catalysts                               |                     |   |    |    |            |               |      |
| 4 Pt-N <sup>b</sup>  | 27                  | — | 28 | 45 | 5.1        | 52            | 48   |
| 5 Pt-N <sup>c</sup>  | 23                  | — | 38 | 39 | 4.8        | 63            | 37   |
| 6 Pt-HCHO-473 <sup>c</sup>                                     | 13                  | 1 | 44 | 42 | 4.5        | 62            | 38   |
| 7 Pt-HCHO-633 <sup>c</sup>                                     | 19                  | 1 | 47 | 33 | 4.5        | —             | —    |
| <i>(c)</i> Pt-HCHO-473 catalyst measured at 600 K <sup>c</sup> |                     |   |    |    |            |               |      |
| 8 heated   | 9                   | 1 | 48 | 42 | 4.4        | 65            | 35   |
| 9 hydrogen treated   | 14                  | 2 | 22 | 62 | 4.8        | 63            | 34   |

<sup>a</sup> Case history: sample 4 was regenerated to sample 1; sample 6 was regenerated to sample 2; sample 7 was regenerated to sample 3. Runs 8 and 9 were carried out with the same Pt as runs 2 and 6, but the sample was removed from UHV between the two series of runs. Corresponding UP spectra: samples 1 and 2 in Fig. 6; samples 4 and 5 in Fig. 7; samples 5 and 6 in Fig. 8; UPS before and after XPS of sample 9 in Fig. 11.

<sup>b</sup> Pristine catalyst. <sup>c</sup> Catalyst after reaction of alkane-hydrogen mixture.



**Fig. 4** UP He I spectra for (a) chemically purified Pt-N [Table 6(a), sample 1] and (b) Pt-HCHO-473 [Table 6(a), sample 2] together with the respective difference spectra related to the reference Pt foil. A spectrum<sup>54</sup> for a Pt foil annealed at 1120 K is included

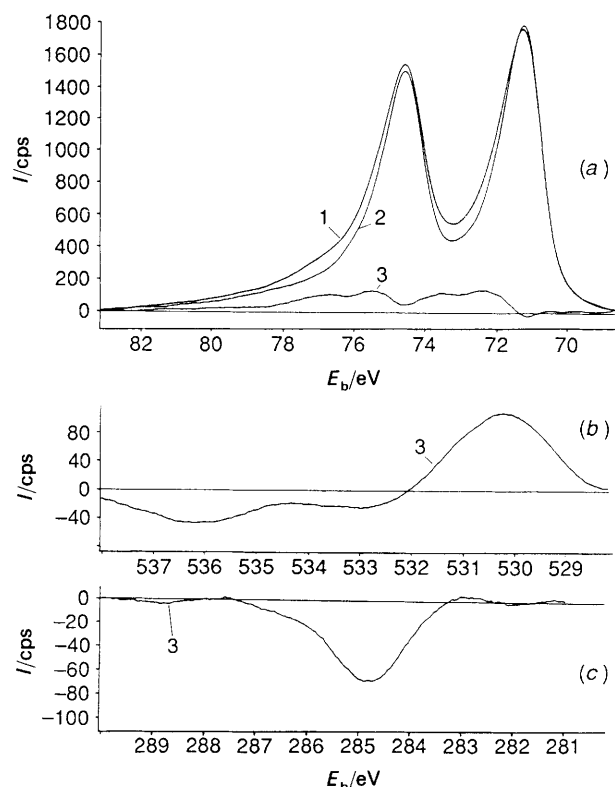


**Fig. 5** (a) Pt 4f region of XP spectra for pristine (curve 1) and used Pt black (curve 2) in the as received state together with their difference spectrum (curve 3 = curve 1 - curve 2). (b) O 1s region. (c) C 1s region. Only the difference spectrum (curve 3) is shown in (b) and (c). Note the different intensity values in (a), (b) and (c)

these assignments are in agreement with XPS (Fig. 3): the O 1s contribution of OH groups and PtO is most intense here. It is not surprising that UPS is a more sensitive method for the detection of a surface PtO adlayer than XPS.

The difference spectrum between the reference Pt and Pt-HCHO-473 shows sharper and more intense bands. A marked feature is seen at 5.2 eV (OH attached to Pt/K sites which are reportedly stable up to 573 K<sup>20</sup>). The broader band centred at 7.5–8 eV contains the contributions of OH/Pt at 7.8 eV, that of water on oxygenated Pt at 8–8.2 eV<sup>38</sup> and the other band<sup>20</sup> of OH on Pt/K at 8.7 eV, together with some PtO bands<sup>21</sup> (6–8 eV) and the hydrocarbon bands.<sup>42,53</sup> The third band between 11 and 13 eV also arises from OH and H<sub>2</sub>O (cf. Table 3). In addition, minor contributions of CO (superimposed) to the broader band at 8–9 eV and also at ca. 12 eV can be recognized. The presence of CO is underlined by the loss of intensity in the Fermi-edge region.<sup>21</sup> This CO may have been incorporated at the moment of the reduction of this sample from the decomposition of HCHO. CO is more clearly seen in UPS than in XPS where its contribution (O 1s  $E_b$  at ca. 531 or 532.8 eV,<sup>21,22</sup> C 1s  $E_b$  at 285.9 eV<sup>15,21</sup>) may overlap with others from oxidized C.

In spite of the significant amount of C detected by XPS, other carbon contributions are not important in UPS. This may indicate a predominantly island-like, 3D carbon structure, where the carbon-metal bonds are located a few atomic layers below the surface. These few atom thick C islands as well as subsurface C (C entities between the grains in crystal aggregates or in cavities shown by the electron micrographs in ref. 9) may also contribute to the XPS signal.

One of the reasons for the difference between the two Pt blacks may be their different K content [Table 6(a)]. One K atom can attract a cluster of several water molecules and/or OH groups<sup>55</sup> and may stabilize OH/H<sub>2</sub>O species produced from the O<sub>2</sub> + H<sub>2</sub> reaction during regeneration of Pt-HCHO (Fig. 4).

The problem of hydrogen present on platinum has to be mentioned. Radiotracer studies have shown that once Pt black is in contact with hydrogen, it remains there even after heating up to 600–700 K in inert gas or during storage in air.<sup>56</sup> Hydrogen decreases the UP intensity near to the Fermi edge; in addition, hydrogen-induced features were reported at 5.8, 6.4 and 7.3 eV, i.e. at positions overlapping with the usually more intense oxygen-containing features.<sup>46</sup> The shape of the UP spectra around the Fermi edge could be interpreted in terms of a surface metal-hydrogen interactions. Annealing Pt(111) after ethene adsorption restored the UPS spectrum of a Pt(111) sample except for the lower intensity at the Fermi edge.<sup>41</sup> This observation points to the possible effect of H atoms split off from hydrocarbons during their dissociative adsorption.<sup>57</sup> This 'invisible' hydrogen may be responsible for several effects which, perhaps, cannot otherwise be explained adequately.

The following sections will discuss briefly three additional areas. These include electron spectroscopy of Pt, in the state before purification (carbonized and/or oxidized Pt) after its regeneration by treatments other than standard regeneration, and electron spectroscopy at high temperatures.

#### Photoelectron Spectroscopy of Oxidized and/or Carbonized Pt Samples: The Way to Purified Pt

Pristine Pt samples after reduction are covered with oxygen and carbon impurities arising from exposure to polluted air.<sup>9,10</sup> Pre-sintering promotes segregation of carbon to the surface.<sup>8</sup> Catalytic hydrocarbon reactions on Pt are accom-

panied with a rapid build-up of a surface carbon layer. A H : C ratio between 1 and 1.5 has been reported for this latter moiety<sup>57</sup> which can be partly removed by interim oxidation. The fraction of irremovable 'residual carbon' was found to be minor.<sup>58</sup>

Although the surface compositions of pristine and used Pt may be close to each other, the main-to-tail ratio in their Pt 4f region is different [Table 6(b)]. Pristine Pt black is oxidized markedly after lengthy storage. This is also confirmed by the relative abundance of the PtO component of the O 1s band, being 11% with pristine Pt [sample 4, Table 6(b)] as opposed to 6% with used Pt [sample 5, Table 6(b)]. The Pt 4f XPS spectrum of the pristine sample [Fig. 5(a)] shows a shoulder at higher  $E_b$ . The difference spectrum shows a negative peak at  $E_b$  71.1 (lower metallic intensity with the pristine Pt) and positive peaks at the higher  $E_b$  tail (higher Pt oxide intensity in the pristine sample, consisting of at least two components). The peak at  $E_b$  = 73.5 eV corresponds to  $\text{Pt}^{2+}$ , while a value at ca 72.4 eV was assumed for  $\text{PtO}_{\text{ads}}$ .<sup>19,33,34</sup> There is no sign of  $\text{Pt}^{4+}$  ( $E_b$  74.1 eV). The O 1s region of the difference spectrum also confirmed the presence of more PtO and less oxidized carbon and/or charged species [Fig. 5(b)] in pristine Pt. Used Pt contains more carbon, in particular, more graphite and  $\text{C}_x\text{H}_y$  polymer [Fig. 5(c)].

The He I spectrum of the pristine Pt-N (Fig. 6) contains bands of surface oxygenates along with a broad carbon peak (curve 1) while only the latter appears with the used Pt-N sample (curve 2). This spectrum is similar to that reported for an a-C : H overlayer<sup>43</sup> (curve 3). Both samples exhibit Fermi-edge intensities higher than zero. Regeneration with  $\text{O}_2$  and  $\text{H}_2$  removes a band centred at 8–9.5 eV from the pristine sample (curve 4) while almost a mirror image of the a-C : H UP spectrum is removed from the catalyst which had been in contact with hydrocarbon reactants (curve 5).

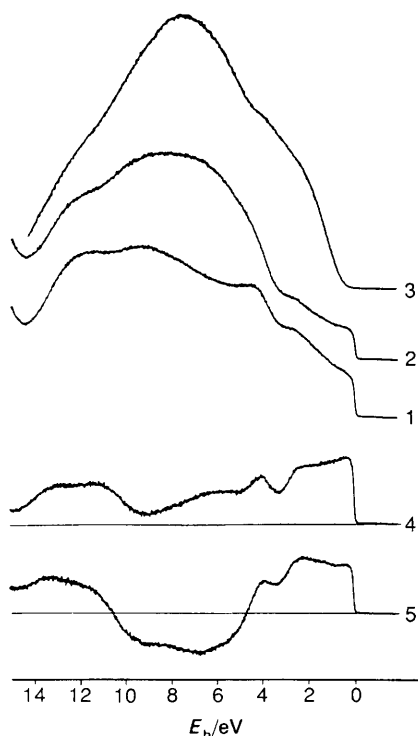


Fig. 6 UP He I spectra for 1, pristine Pt-N [sample 4, Table 6(b)] and 2, used Pt-N (after *n*-hexane reaction) [sample 5, Table 6(b)] in the as received state. Curve 3 is a spectrum for a-C : H.<sup>43</sup> Curves 4 and 5 are difference spectra: 4, (regenerated pristine Pt-N) – (curve 1); 5, (regenerated used Pt-N) – (curve 2)

Fig. 7 depicts analogous He II UP spectra. Samples used in hydrocarbon reactions show a 'double buckle' similar to that reported for oxidized diamond.<sup>25</sup> The total length of the catalytic runs of Pt-N was much shorter than with Pt-HCHO-473, which is the reason why the intensity of the C peak of the former is also lower. The small Fermi edge demonstrates that a minor fraction of even a contaminated disperse catalyst is in a chemically pure metallic state (island-like overlayer), as opposed to the Pt foil where, owing to a similar amount of impurity [cf. Tables 5 and 6(b)], no Fermi edge appears (contiguous overlayer).

The similarity between the shape of UP spectra of a-C : H overlayers and that arising from carbon on Pt blacks is remarkable. Another argument is supplied by the considerable amount of ' $\text{C}_x\text{H}_y$ ' polymer in the C 1s line fitting. As XPS (Fig. 3) and UPS (Fig. 6 and 7) demonstrate, this layer is in a partly oxidized state. The growth of a considerable a-C : H overlayer on Ni causes no appreciable shift of the Ni core level  $E_b$  (i.e. no electronic interaction could be detected between C and the underlying metal); also, a relatively facile transition was reported between atomic C, graphite, glassy carbon and a-C : H, the species appearing on Ni under identical conditions in the above sequence.<sup>29</sup> A much thinner graphite layer preceded a-C : H formation on Pt.<sup>15</sup> Two more facts can be recalled from the literature. An ordered overlayer transformed into a disordered one when a mixture of hydrogen and hydrocarbon reacted on a Pt single crystal which might have corresponded to a graphite → a-C : H transformation.<sup>59</sup> Secondly, a compact carbonaceous skin was left behind when Pt black covered with segregated carbon was sintered under the beam of an electron microscope.<sup>8</sup> Electron diffraction showed graphite, amorphous carbon and some unidentified substance, the reflections of which do not exclude a-C : H although its presence was not

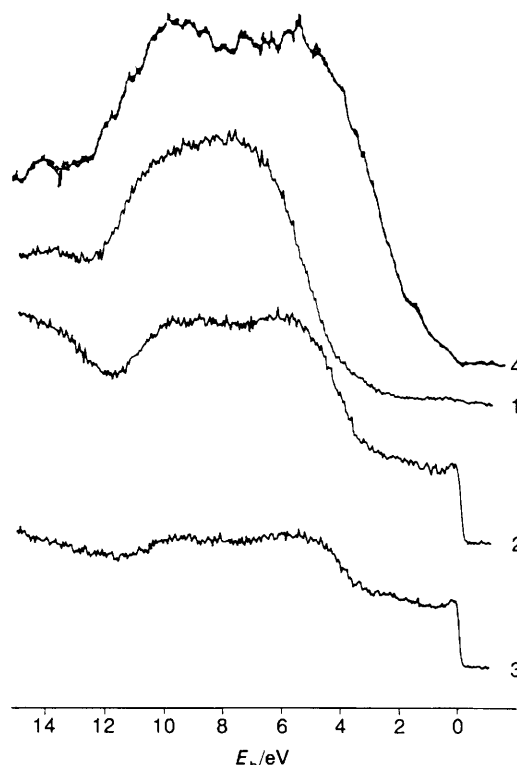


Fig. 7 He II UP spectra of 1, Pt foil, 2, Pt-HCHO-473 sample 6, Table 6(b) and 3, Pt-N sample 5, Table 6(b) in the as received state. Both Pt blacks were used in hydrocarbon reactions previously. 4, UP He II spectrum for oxidized diamond<sup>25</sup> shown for comparison



concluded at that time. Fibrous spiralled graphitic<sup>60</sup> and three-dimensional amorphous carbon<sup>61</sup> were also detected on Pt black by electron microscopy. The problem of formation of a-C:H under these atypical conditions would certainly be worth investigating.

#### Photoelectron Spectroscopy of Pt Black after various Regenerative Treatments

The conditions of standard regeneration to purify Pt black have been selected on an empirical basis.<sup>7</sup> The data presented so far indicate the incompleteness of carbon removal by this procedure. Attempts were made to apply repeated or more severe regeneration to find out whether Pt black purification could be made more complete. Pt-HCHO-633 [line 3 in Table 6(a)] was selected for this purpose where pre-sintering produced larger crystallites,<sup>9</sup> additional sintering seemed, therefore, less likely. All treatments followed each other in the sequence given in Table 7, without taking the sample out of the UHV chamber.

Even repeated or high-temperature oxidation could not decrease the carbon content of Pt black below 18–20%. At the same time, the amount of oxygen increased to 22–29%. The impact of these treatments on catalytic properties is published elsewhere.<sup>62</sup>

Selected XP and UP spectra (after treatments B, E, F) demonstrate that although the amounts of surface oxygen and carbon may be close, their chemical form is different. The C 1s lines [Fig. 8(a)] are rather similar after various treatments. Small carbide peaks ( $E_b$  around 283 eV) due to carbon segregation at high temperatures<sup>8</sup> are removed by hydrogen only (E). High-temperature oxygen treatment (F) increases the carbonyl peak at  $E_b$  around 288 eV.

PtO ( $E_b$  just above 530 eV) appears as a pronounced shoulder after B and F [Fig. 8(b)]. As opposed to broad bands after standard regeneration (sorbed water patches), hydrogenation at 600 K (E) and at 700 K (D) produces sharp UPS features indicating individual OH adspecies on Pt as well as Pt/K sites [Fig. 8(c)]. This treatment produced a metallic state as clean as that of the reference foil (no Fermi-edge intensity difference). Note the shift of band positions after F to  $E_b$  4.5 and 6 eV indicating the presence of surface O species rather than OH groups, in agreement with XPS results [cf. Fig. 8(b) and (c)]. The increased work function values (Table 7) can also be attributed to the presence of surface oxygen.

#### Photoelectron Spectroscopy of Pt Black at High Temperatures

Heating any Pt black up to 600 K in UHV removes some of its oxygen content [Table 6(c)]. The intensity of the O 1s

**Table 7** Composition of Pt-HCHO-633 after various regenerative treatments

| sample                                | composition (atom%) |     |    |      | $\Phi$ /eV |
|---------------------------------------|---------------------|-----|----|------|------------|
|                                       | O                   | K   | C  | Pt   |            |
| A Pt black, untreated                 | 19                  | 0.4 | 47 | 33.5 | 4.5        |
| B normal regen., 603 K                | 18                  | 1.7 | 29 | 51   | 4.4        |
| C As B, 4 times                       | 27                  | 2   | 18 | 53   | 4.4        |
| D As B, at 693 K                      | 24                  | 2   | 20 | 54   | 4.4        |
| E H <sub>2</sub> , 603 K, 2 times     | 22                  | 1.6 | 19 | 58   | 4.5        |
| F O <sub>2</sub> , 800 K <sup>a</sup> | 28                  | 1.8 | 21 | 49   | 4.8        |
| G H <sub>2</sub> , 750 K <sup>b</sup> | 24                  | 2.2 | 23 | 51   | 4.4        |

All data have been rounded to whole number except for K where concentration changes of a few tenths of a per cent can be instructive. <sup>a</sup> 10 min, 13 mbar. <sup>b</sup> 1 min, 133 mbar.

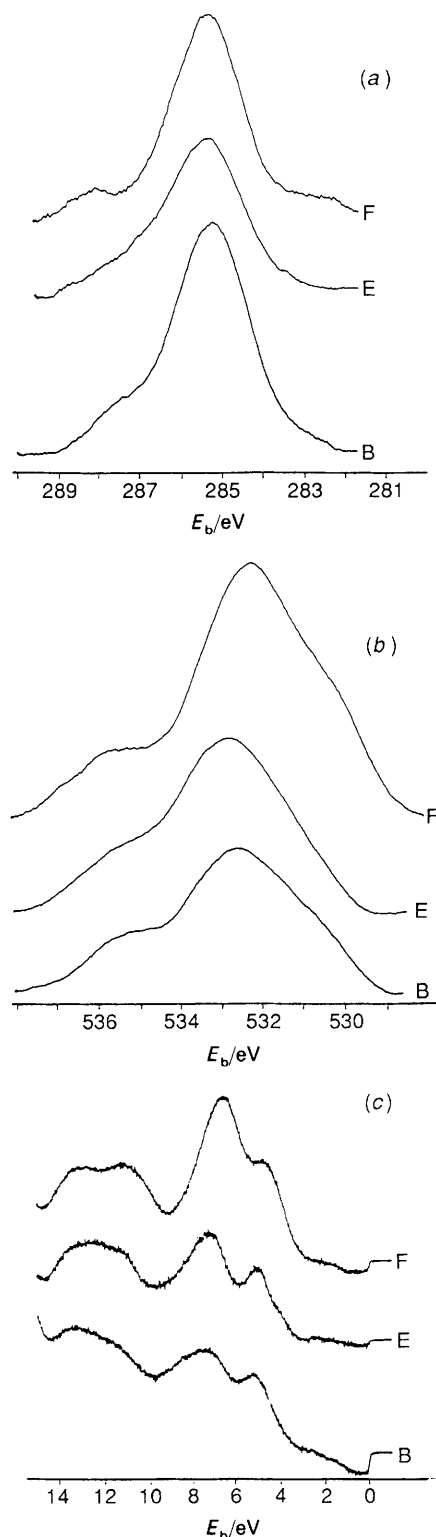


**Fig. 8** Selected XPS lines for Pt-HCHO-633 after treatments B, E, F (see Table 7). (a) C 1s; (b) O 1s; (c) Difference He I UP spectra with the reference Pt foil (B - case 2, E - case 2, F - case 2)

band decreased, that of C 1s increased. The decrease was most pronounced in the Pt-OH and H<sub>2</sub>O region of O 1s. The intensity growth at 284 eV indicated a commencing graphitization of the hydrocarbon polymer. The presence of PtC increased due to carbon segregation.<sup>8</sup> UP spectra show essentially the same features as shown in Fig. 6 and 7. Hence, mere heating can be regarded as a rather inefficient way of Pt purification.

In one run, XP spectra were measured at 603 K, prior to and following a 603 K hydrogen treatment. This treatment increased the Pt intensity and produced just as clean a surface as observed after normal regeneration [cf. Tables 6(a) and (c)]. The main-to-tail ratio [Table 6(c)] indicates also some Pt oxidation, in agreement with O 1s fitting and the asymmetric increase of the oxide/OH region in the difference spectrum [Fig. 9A]. The carbon contributions are removed almost uniformly [Fig. 9B].

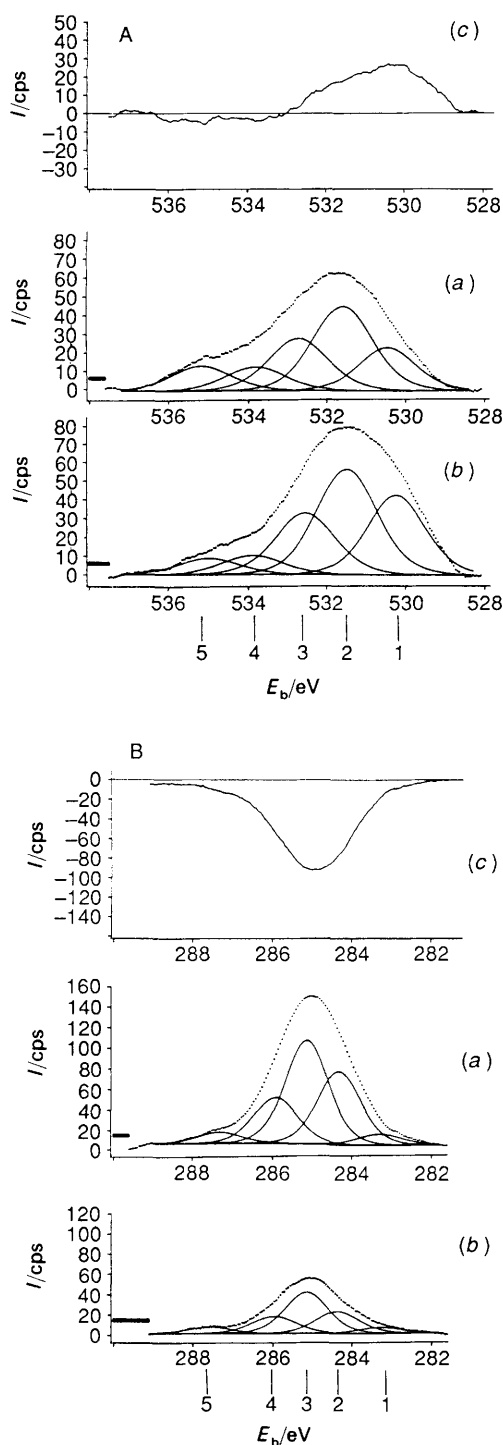


**Fig. 9** XP spectra for Pt-HCHO-473 measured at 600 K. (a) after hydrogen treatment [Table 6(c), sample 9]; (b) before hydrogen treatment [Table 6(c), sample 9]; (c) difference spectra, (a) – (b). Assignments: A, O 1s line: 1, PtO; 2, OH; 3, H<sub>2</sub>O; 4, oxidized carbon; 5, charged species (condensed water); B, C 1s line: 1, PtC; 2, graphite; 3, C<sub>x</sub>H<sub>y</sub> polymer; 4, oxidized C; 5, charged species

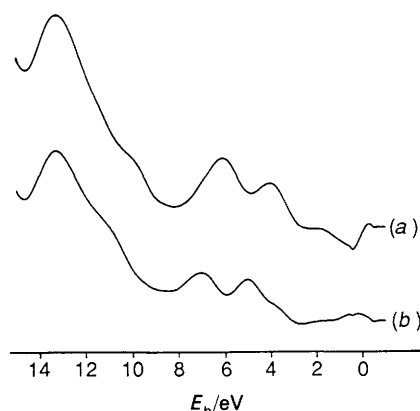


**Fig. 10** Difference He I UP spectra between the reference Pt foil of Fig. 3 and Pt-HCHO-473 measured at 603 K (a), 15 min and (b) 16 h after hydrogen treatment [Table 6(c), sample 9]

The He I UP spectrum measured directly after contact with H<sub>2</sub> [Fig. 10(a)] shows a band at ca. 4–4.5 eV which appears also on curve E in Fig. 8(c). This may correspond to OH/K species,<sup>20</sup> to the 2p band of segregated C atoms<sup>63</sup> or to hydrogen-induced surface reconstruction as reported for Pt foil<sup>54</sup> and single crystal.<sup>64</sup> Another band appears at ca. 6 eV, which can be assigned to O<sup>–</sup> (surface Pt oxide and/or the chemisorbed overlayer). The OH<sup>–</sup> and PtO assignments are supported by the XP spectrum of Fig. 10(a).

It may be surprising that *hydrogen* treatment enhances a surface oxygen feature. However, the same phenomenon was also observed with Pd black<sup>12</sup> where hydrogen atoms penetrating into subsurface layers pushed subsurface oxygen atoms to the surface, which themselves could be detected by photoelectron spectroscopy. Three additional arguments can be put forward. (i) Hydrogen penetration below the surface of platinum has been demonstrated.<sup>56,65</sup> (ii) The He I spectrum of the same sample exposed to air at 300 K produced similar UP spectrum as seen in Fig. 10(a). (iii) The work function immediately after high-temperature hydrogen treatment is equal to the value observed after a high-temperature oxygenation [cf. Tables 6(c) and 7] and this value is re-established after the procedure mentioned under (ii).

During an overnight XPS experiment carried out at 603 K, most of the above features disappeared except for a small shoulder at  $E_b = 4.5$  eV [Fig. 10(b)]. Surface oxygen and subsurface hydrogen species must, therefore, have reacted to give H<sub>2</sub>O and the remaining OH groups distributed over pure Pt and Pt/K sites. The coexistence of sorbed O and H at ca. 300 K for several minutes has been demonstrated;<sup>40</sup> the present observation shows that the reaction O + H may not be instantaneous even at 600 K. The C atoms (if present) were polymerized and surface reconstruction annealed.

## Conclusions

Photoelectron spectroscopy supplies the following experimental evidence on the catalyst surface:

(i) The surface of a Pt black is predominantly in a clean metallic state not inferior to clean reference Pt upon customary catalyst regeneration with O<sub>2</sub> and H<sub>2</sub> at 600 K, although this surface contains impurities. In other words, metallic Pt and clean Pt are not necessarily synonymous. In spite of its marked effect in surface purification, and contrary to general belief, *hydrogen does not remove all surface oxygen*. It creates, instead, OH/H<sub>2</sub>O species attached to the metallic sites. These are stable for at least several h at ca. 600 K in UHV. The presence of K on Pt stabilizes these moieties but

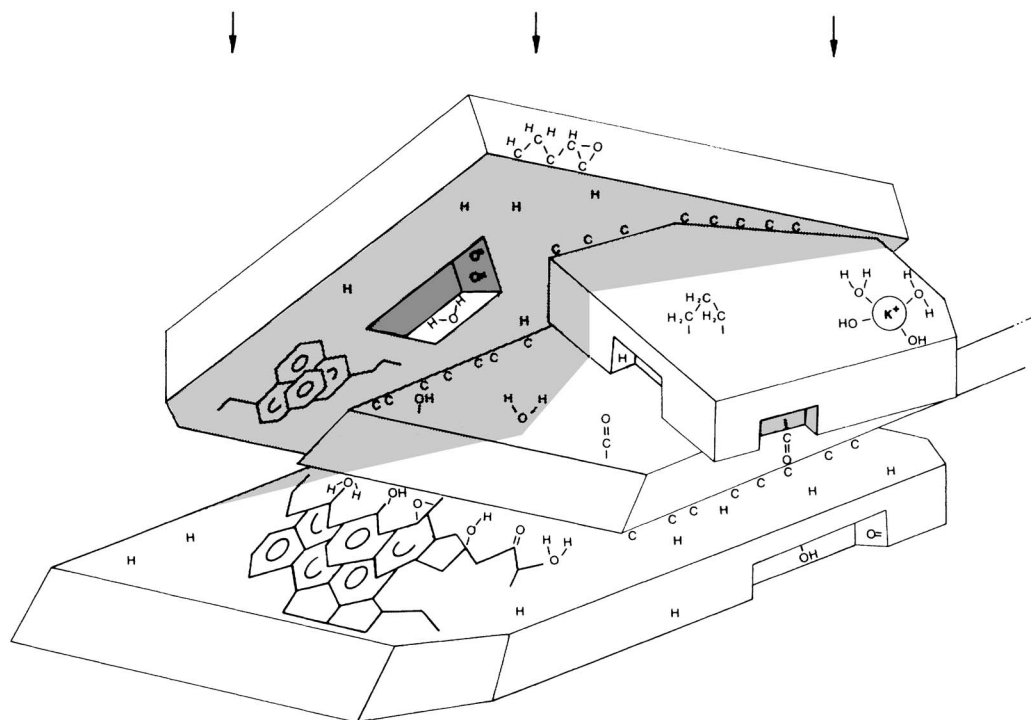


**Fig. 11** An artist's impression of the purified Pt surface. Various surface species detected are shown. The likely C enrichment along grain boundaries is shown schematically. The arrows denote the incidence of excitation for electron spectroscopy. Species that are situated in the shadow of the incident beam (shaded areas or in cavities) may be within the information depth of XPS, hence they are detected by that method but are undetectable by UPS

potassium cannot hold the entire responsibility for their presence.

(ii) The surface of a pristine Pt is largely oxidized. Pt oxide is reduced by  $H_2$  treatments and is displaced by carbonaceous overlayers (resembling a-C:H) after hydrocarbon reactions. Regeneration removes *ca.* half of those 2-D carbon impurities. The remaining carbon exhibits an island-like 3-D structure (with graphitic and  $C_xH_y$  polymer components). These are partly oxidized. Sorbed CO represents, likely, a minor fraction of surface carbon.

(iii) All these species can be present also in cavities, along interparticle boundaries, *i.e.* hidden from detection in a three-dimensional loose stacking of crystallites. Fig. 11 shows an artist's impression of the surface, illustrating also these true and apparent subsurface species.

### Implications of Results of Surface Analysis for Catalysis

The presence of pure metal islands, single carbon atoms attached to metal atoms and 3D carbonaceous overlayers on Pt single crystals was postulated<sup>4,66</sup> under the conditions of hydrocarbon catalysis. Catalytic activity was attributed to the first two types of site. Most skeletal hydrocarbon reactions are claimed to require clean Pt sites<sup>57</sup> whereas Pt-C ensembles can catalyse, for example, terminal C-C bond splitting<sup>67,68</sup> or dehydrogenation reactions.<sup>68</sup> Hardly any PtC species can be detected by the present set-up. The above changes in catalytic selectivities indicate their formation. These species are removed by controlled oxidation.<sup>69</sup> They do not seem to survive contact with air, when the catalyst is taken out of the reactor. The quinone/aroxyl structures of a 3D carbonaceous deposit were claimed to possess redox properties,<sup>31</sup> thus they can contribute to dehydrogenation reactions.

As far as metallic Pt sites are concerned, the first portions of any hydrocarbon reactant meet a Pt/OH/ $H_2O$  surface

instead of a pure metal. Degradative reactions, predominantly to methane, prevailed when *n*-hexane was reacted over an oxidized Pt single crystal<sup>57</sup> or over Pt black pretreated with oxygen.<sup>70</sup> The presence of oxygenates may induce an initial predominating degradative activity of Pt.

High methane selectivity is observed at low conversions of *n*-hexane over Pt-HCHO-473 regenerated a few times in sequence (Table 8). Non-degradative products also appear at higher conversions. No evidence is available as to whether oxygenates on Pt participate directly in catalytic hydrogenolysis or their effect is indirect, and can be attributed, *e.g.* to hindering the formation of Pt-C-H entities that are necessary for non-degradative reactions.<sup>68,69,71-73</sup>

The presence of oxygen-containing surface species may have consequences also in catalyst characterization. Exact stoichiometries of the hydrogen-oxygen titration widely used for determination of metallic surface are still controversial.<sup>65</sup> Water has been reported to leave the Pt surface,<sup>74,75</sup> however, the presence of surface PtOH and also the possible effect of K impurity have been considered.<sup>74</sup> *Ca.* 20% of

**Table 8** Selectivity of *n*-hexane reaction over Pt-HCHO-473 at various conversion levels<sup>a</sup>

| conversion (%) | selectivity (%) <sup>b</sup> |                                |                                  |                 |                 |
|----------------|------------------------------|--------------------------------|----------------------------------|-----------------|-----------------|
|                | CH <sub>4</sub>              | C <sub>2</sub> -C <sub>5</sub> | C <sub>6</sub> sat. <sup>c</sup> | Ol <sup>d</sup> | Bz <sup>d</sup> |
| 0.7            | 72.7                         | 11.1                           | 16.2                             | 0               | 0               |
| 1.4            | 38.7                         | 11.1                           | 49.9                             | 0               | 0               |
| 6.1            | 18.4                         | 16.5                           | 57.0                             | 1.1             | 6.9             |
| 24.7           | 10.8                         | 19.5                           | 52.5                             | 0.4             | 16.8            |

<sup>a</sup> Static-circulation reactor, 84 mg catalyst,  $T = 603$  K,  $p(H_2) = 160$  mbar,  $p(n\text{-hexane}) = 13.3$  mbar. <sup>b</sup> Calculated from the amount of hexane molecules transformed to the respective products. <sup>c</sup> Isomers (2-methylpentane plus 3-methylpentane) and methylcyclopentane. <sup>d</sup> Ol = *n*-hexene isomers; Bz = benzene.

adsorbed O became unreactive towards hydrogen after heating Pt to 573 K.<sup>76</sup> O atoms in subsurface positions were then assumed; here we have shown that surface species (OH and H<sub>2</sub>O) may also be stable. Our direct confirmation of the presence of surface OH/H<sub>2</sub>O entities may open up new interpretation possibilities for discrepancies, e.g. dependence of the H<sub>2</sub> and O<sub>2</sub> titration stoichiometry on the number of cycles, 'loss' and 'recovery' of surface Pt etc.<sup>65,74</sup>

If the presence of OH groups on metallic sites is a typical phenomenon rather than an exception, it would be worth considering their effect in hydrogen spillover, since interactions between H atoms on metallic and OH groups on support sites have been assumed in that process.<sup>77</sup>

Helpful discussions with Dr M. Kiskinova and Prof. H. P. Bonzel as well as with Prof. G. Maire are gratefully acknowledged.

## References

- 1 T. L. Barr, in *Practical Surface Analysis*, ed. D. Briggs and M. P. Seah, Wiley, Chichester, 1983, p. 283.
- 2 G. Ertl, and J. Küppers, *Low Energy Electrons and Surface Chemistry*, Verlag Chemie, Weinheim, 1974.
- 3 H. P. Bonzel, *Surf. Sci.*, 1977, **68**, 236.
- 4 Z. Paál and P. Tétényi, in *Catalysis Specialists Periodical Reports*, ed. G. C. Bond and G. Webb, Royal Society of Chemistry, London, 1982, p. 80.
- 5 S. M. Davis, F. Zaera and G. A. Somorjai, *J. Catal.*, 1984, **85**, 206.
- 6 F. Garin, S. Aiyeach, P. Légaré and G. Maire, *J. Catal.*, 1982, **77**, 323.
- 7 H. Zimmer, M. Dobrovolsky, P. Tétényi and Z. Paál, *J. Phys. Chem.*, 1986, **90**, 4758.
- 8 A. Barna, P. B. Barna, L. Tóth, Z. Paál, P. Tétényi, *Appl. Surf. Sci.*, 1982–83, **14**, 85.
- 9 Z. Paál, H. Zimmer, J. R. Günter, R. Schlögl and M. Muhler, *J. Catal.*, 1989, **119**, 146.
- 10 Z. Paál, P. Tétényi, D. Prigge, X. Zh. Wang and G. Ertl, *Appl. Surf. Sci.*, 1982–83, **14**, 307.
- 11 Z. Paál, D. Marton, *Appl. Surf. Sci.*, 1986, **26**, 161.
- 12 K. Noack, H. Zbinden and R. Schlögl, *Catal. Lett.*, 1990, **4**, 145.
- 13 Z. Paál, G. Loose, G. Weinberg, M. Rebholz and R. Schlögl, *Catal. Lett.*, 1990, **6**, 301.
- 14 Z. Paál and R. Schlögl, *Surf. Interface Anal.*, in the press.
- 15 R. Schlögl, *Surf. Sci.*, 1987, **189/190**, 861.
- 16 D. N. Belton and S. J. Schmieg, *Surf. Sci.*, 1990, **233**, 131.
- 17 P. Légaré, L. Hilaire and G. Maire, *Surf. Sci.*, 1984, **141**, 604.
- 18 W. Ranke and H. J. Kuhr, *Phys. Rev. B*, 1989, **39**, 1595.
- 19 M. Peuckert and H. P. Bonzel, *Surf. Sci.*, 1984, **145**, 239.
- 20 M. Kiskinova, G. Pirug and H. P. Bonzel, *Surf. Sci.*, 1985, **150**, 319.
- 21 M. Kiskinova, G. Pirug and H. P. Bonzel, *Surf. Sci.*, 1983, **133**, 321.
- 22 P. R. Norton, *Surf. Sci.*, 1975, **47**, 98.
- 23 S. G. Anderson, H. M. Meyer III and J. H. Weaver, *J. Vac. Sci. Technol., A*, 1988, **6**, 2205.
- 24 S. Akhter, X.-L. Zhou and J. M. White, *Appl. Surf. Sci.*, 1989, **37**, 201.
- 25 S. Evans and J. M. Thomas, *Proc. R. Soc. London, A*, 1977, **353**, 103.
- 26 R. Schlögl and H. P. Boehm, *Carbon*, 1983, **21**, 345.
- 27 N. Freyer, G. Pirug and H. P. Bonzel, *Surf. Sci.*, 1983, **126**, 487.
- 28 C. Benndorf, M. Grischke, H. Koeberle, R. Menning, A. Brauer and F. Thieme, *Surf. Coat. Technol.*, 1988, **36**, 171.
- 29 D. N. Belton and S. J. Schmieg, *J. Appl. Phys.*, 1989, **63**, 4223.
- 30 S. Akhter, K. Allan, D. Buchanan, J. A. Cook, A. Campoin and J. M. White, *Appl. Surf. Sci.*, 1988–89, **35**, 241.
- 31 A. Schraut, G. Emig and H.-G. Sockel, *Appl. Catal.*, 1987, **29**, 311.
- 32 S. Doniach and P. Sunjic, *J. Phys., C*, 1970, **3**, 285; a Pt spectrum is shown by D. Briggs and J. C. Rivière, in *Practical Surface Analysis*, ed. D. Briggs and M. P. Seah, Wiley, Chichester, 1983, p. 132.
- 33 K. S. Kim, N. Winograd and R. E. Davis, *J. Am. Chem. Soc.*, 1971, **93**, 6296.
- 34 T. Dickinson, A. F. Povey and P. M. A. Sherwood, *J. Chem. Soc., Faraday Trans. 1*, 1975, **71**, 298.
- 35 J. Küppers and G. Ertl, *Surf. Sci.*, 1978, **77**, L647.
- 36 A. Slavin, J. Fusy, J. Jupille, M. Alnot, J. J. Ehrhardt and A. Cassuto, *Proc. 4 ICSS and 3 ECOSS, Suppl. Le Vide, les Couches Minces*, No. 201, vol. 1, p. 510.
- 37 J. L. Gland, B. A. Sexton and G. B. Fisher, *Surf. Sci.*, 1980, **95**, 587.
- 38 G. B. Fisher and B. A. Sexton, *Phys. Rev. Lett.*, 1980, **44**, 683, 595.
- 39 H. P. Bonzel, G. Pirug and A. Winkler, *Surf. Sci.*, 1986, **175**, 287.
- 40 P. R. Norton, in *The Chemical Physics of Solid Surfaces and Heterogeneous Catalysis*, ed. D. A. King and D. P. Woodruff, Elsevier, Amsterdam, 1982, vol. 4, p. 27.
- 41 M. B. Hugenschmidt, P. Dolle, J. Jupille and A. Cassuto, *J. Vac. Sci. Technol., A*, 1989, **7**, 3312.
- 42 M. G. Ramsey, G. Rosina, D. Steinmueller, H. H. Graen and F. P. Netzer, *Surf. Sci.*, 1990, **232**, 263.
- 43 M. E. Wittmer, D. Ugolini and P. Oelhafen, *J. Electrochem. Soc.*, 1990, **137**, 1256.
- 44 R. C. White, R. Haight, B. D. Silverman and P. S. Ho, *Appl. Phys. Lett.*, 1987, **51**, 481.
- 45 T. Schedel-Niedrig, H. Sotobayashi, A. Ortega-Villamil and A. M. Bradshaw, *Surf. Sci.*, 1991, **247**, 83.
- 46 J. E. Demuth, *Surf. Sci.*, 1977, **65**, 369.
- 47 H. P. Bonzel and G. Pirug, *Surf. Sci.*, 1977, **62**, 45.
- 48 H. H. Rotermund, S. Jakubith, S. Kubala, A. von Oertzen and G. Ertl, *J. Electron Spectrosc. Rel. Phenom.*, 1990, **52**, 811.
- 49 R. Hauert, Dissertation, Basel, 1986.
- 50 H. Conrad, J. Küppers, F. Nitschke and F. P. Netzer, *J. Catal.*, 1978, **52**, 186.
- 51 J. Küppers and G. Ertl, *Surf. Sci.*, 1978, **72**, L647.
- 52 H. P. Bonzel, G. Brodén and H. J. Krebs, *Appl. Surf. Sci.*, 1983, **16**, 373.
- 53 G. Brodén, T. Rhodin and W. Capehart, *Surf. Sci.*, 1976, **61**, 143.
- 54 D. M. Collins and W. E. Spicer, *Surf. Sci.*, 1977, **69**, 114.
- 55 M. Kiskinova and H. P. Bonzel, personal communication.
- 56 Z. Paál and S. J. Thomson, *J. Catal.*, 1973, **30**, 96.
- 57 G. A. Somorjai, in *The Chemical Physics of Solid Surfaces and Heterogeneous Catalysis*, ed. D. A. King and D. P. Woodruff, Elsevier, Amsterdam, 1982, vol. 4, p. 217.
- 58 F. Garin, G. Maire, S. Zyade, M. Zauwen, A. Frennet and P. Zielinski, *J. Mol. Catal.*, 1990, **58**, 185.
- 59 D. W. Blakely and G. A. Somorjai, *J. Catal.*, 1976, **42**, 181.
- 60 J. R. Fryer and Z. Paál, *Carbon*, 1973, **11**, 635.
- 61 Z. Paál, J. R. Fryer, and S. J. Thomson, in *Symposium on the Mechanisms of Hydrocarbon Reactions*, ed. F. Márta and D. Kalló, Akadémiai Kiadó, Budapest, 1975, p. 137.
- 62 Z. Paál, R. Schlögl and G. Ertl, *Catal. Lett.*, 1992, **12**, 331.
- 63 S. J. Atkinson, C. R. Brundle and M. W. Roberts, *Faraday Discuss. Chem. Soc.*, 1974, **58**, 62.
- 64 H. P. Bonzel, C. R. Helms, S. Kelemen, *Phys. Rev. Lett.*, 1975, **35**, 1237.
- 65 Z. Paál and P. G. Menon, *Catal. Rev.-Sci. Eng.*, 1983, **25**, 229.
- 66 S. M. Davis, F. Zaera and G. A. Somorjai, *J. Catal.*, 1982, **77**, 439.
- 67 V. Ponec, *Adv. Catal.*, 1983, **32**, 149.
- 68 Z. Paál, I. Manninger, Zh. Zhan and M. Muhler, *Appl. Catal.*, 1990, **63**, 305.
- 69 A. Sárkány, *J. Chem. Soc., Faraday Trans. 1*, 1988, **84**, 2267.
- 70 E. Santacesaria, D. Gelosa and S. Carrà, *J. Catal.*, 1975, **39**, 403.
- 71 A. Sárkány, *J. Chem. Soc., Faraday Trans. 1*, 1989, **85**, 1523.
- 72 Z. Paál, H. Groeneweg and J. Paál-Lukács, *J. Chem. Soc., Faraday Trans. 1*, 1990, **86**, 3159.
- 73 Z. Paál, *Catal. Today*, in the press.
- 74 D. J. O'Rear, D. G. Löffler and M. Boudart, *J. Catal.*, 1990, **121**, 131.
- 75 B. Sen and M. A. Vannice, *J. Catal.*, 1991, **129**, 31.
- 76 M. Akhtar and F. C. Tompkins, *Trans. Faraday Soc.*, 1971, **67**, 454.
- 77 W. Curtis Conner Jr., in *Hydrogen Effects in Catalysis*, ed. Z. Paál and P. G. Menon, Marcel Dekker, New York, 1988, p. 311.